Thermal Conductivity of Binary Aqueous NaBr and KBr and Ternary H_2O + NaBr + KBr Solutions at Temperatures from (294 to 577) K and Pressures up to 40 MPa

Ilmutdin M. Abdulagatov,*,†,‡ Lala A. Akhmedova-Azizova,§ and Nazim D. Azizov§

Institute for Geothermal Problems of the Dagestan Scientific Center of the Russian Academy of Sciences, 367003 Shamilya Str. 39-A, Makhachkala, Dagestan, Russia, and Azerbaijan State Oil Academy, Baku, 370601, Azerbaijan

The thermal conductivity of four binary aqueous NaBr solutions of (10, 20, 30, and 38) mass %, three binary aqueous KBr solutions of (10, 20, and 30) mass %, and three ternary aqueous NaBr + KBr solutions of (10NaBr + 5KBr, 10NaBr + 10KBr, and 10NaBr + 20KBr) mass % have been measured with a concentric-cylinder (steady-state) technique. Measurements were made near the saturation curve of (0.1 to 2) MPa and at two isobars of (10 and 40) MPa. The range of temperature was (294 to 577) K. The total uncertainty in the thermal conductivity, pressure, temperature, and composition measurements was estimated to be less than 2%, 0.05%, 30 mK, and 0.02%, respectively. The temperature, pressure, and concentration dependence of the thermal conductivity of binary and ternary solutions were studied. The measured values of thermal conductivity were compared with data and correlations reported in the literature. The reliability and accuracy of the experimental method was confirmed with measurements on pure water with well-known thermal conductivity values. The experimental and calculated values of thermal conductivity for pure water from the IAPWS formulation show excellent agreement within their experimental uncertainties (AAD within 0.51%) in the temperature range from (290 to 575) K and at pressures up to 40 MPa. Correlation equations for the thermal conductivity of the binary solutions studied were obtained as a function of temperature, pressure, and composition by a least-squares method from the experimental data. The AAD between measured and calculated values from this correlation for the thermal conductivity was 1.5%.

Introduction

Transport properties, particularly the thermal conductivity of aqueous electrolyte solutions, are useful in many industrial and scientific applications such as the chemical industry, desalination processes, geochemistry, calculation of design parameters, development and utilization of geothermal and ocean thermal energy, geology and mineralogy, hydrothermal synthesis, and in the prediction of heat- and mass-transfer coefficients. To understand and control those processes that used electrolyte solutions, it is necessary to know their thermodynamic and transport properties. The properties of electrolyte solutions are also important for environmental and regulatory-related applications. The treatment of wastewater and flue and vent gases often requires accurate electrolyte solution properties data. The thermal conductivity of electrolyte solutions is also a research interest because the long-range electrostatic interactions presented cause difficulty in describing such systems. Available theoretical models still cannot treat real system as they are met in practice. (For example, complex ionic solutions are extremely difficult.) Better predictive models should be developed on the basis of reliable experimental information on thermodynamic and transport properties data. However, measurements of the thermal conductivity of aqueous salt solutions have so far been limited to rather narrow ranges of temperature, pressure, and concentration with less satisfactory accuracy.

The main objective of the paper is to provide new accurate experimental thermal conductivity data for binary H_2O + NaBr and H_2O + KBr and ternary H_2O + NaBr + KBr solutions at high temperatures (up to 577 K) and high pressures (up to 40 MPa) for compositions up to 40 mass %. The present results considerably expand the temperature, pressure, and concentration ranges in which thermal conductivity data for aqueous NaBr, KBr, and NaBr + KBr solutions are available. This work is part of a continuing program on the transport properties (thermal conductivity and viscosity) of electrolytes in aqueous solutions. In previous studies,[1−15] we measured the thermal conductivity of 30 aqueous salt solutions at high temperatures (up to 573.15 K) and high pressures (up to 100 MPa) using coaxial cylinders and parallel-plate techniques. Thermal conductivity for the binary H_2O + NaBr and H_2O + KBr solutions has been previously studied by several authors.[10,16−28] Table 1 shows all available thermal conductivity data sets for binary H_2O + NaBr and H_2O + KBr solutions. In this Table, the first author is given together with the method employed, the uncertainty of the measurements, and the temperature, pressure, and concentration ranges. Some of the reported thermal conductivities are inaccurate and inconsistent. As one can see from Table 1, three methods (coaxial cylinders, parallel plate, and transient hot-wire) were employed to measure the thermal conductivity of binary H_2O + NaBr and H_2O + KBr solutions. A literature

* Corresponding author. E-mail: ilmutdin@boulder.nist.gov.
† Dagestan Scientific Center of the Russian Academy of Sciences.
‡ Present address: Physical and Chemical Properties Division, National Institute of Standards and Technology, 325 Broadway, Boulder, Colorado 80305.
§ Azerbaijan State Oil Academy.

10.1021/je049814b CCC: $27.50
Published on Web 09/10/2004

Table 1. Summary of the Thermal Conductivity Measurements for Aqueous NaBr and KBr Solutions

first author	year	T/K	P/MPa	100ω/mass %	method	uncertainty/%	salt
Rastorguev[16]	1984	293−473	100	3−15	CC[a]	1.2 to 1.5	NaBr
Abdulagatov[10]	2001	293−473	100	2.5−25	PP	1.6	KBr
Eldarov[17]	1986	293−473	30	0−50	CC	1.8	NaBr
Abdullaev[18]	1981	293−473	30	0−50	CC	2.0	KBr
Magomedov[19]	1989	293−603	100	15−23	PP	1.6	NaBr
Safronov[20]	1990	293−473	100	4.4−19.7	CC	1.5	KBr
Safronov[21]	1990	293−473	100	5−10	CC	1.5	NaBr
							KBr
Zaytsev[23,24]	1998	293−473	0.1	0−40	PP	na	NaBr
			0.1				KBr
Riedel[25]	1951	293	0.1	5−40	CC, PP	1.0	NaBr
				5−50			KBr
Kapustinskii[26]	1955	273−398	0.1	2−50	PP	0.1	NaBr
							KBr
Vargaftik[27]	1956	293−303	0.1	0−20	THW	na	KBr
this work	2004	294−577	40	10−38	CC	2.0	NaBr
				10−30			KBr

[a] CC, coaxial cylinders; PP, parallel plate; THW, transient hot wire; na, no uncertainty given in source reference.

survey revealed that there are no thermal conductivity data for ternary aqueous NaBr + KBr solutions.

Abdulagatov and Magomedov[10] reported thermal conductivity data for H_2O + KBr solutions at pressures from (0.1 to 100) MPa, at temperatures from (293.15 to 473.15) K, and at compositions between (2.5 and 20.0) mass %. Measurements were made by means of the parallel-plate technique. The uncertainty in the thermal conductivity measurements was about 1.6%. Magomedov[17] used same technique to measure the thermal conductivity of H_2O + NaBr solutions in the same temperature, pressures, and concentration ranges. The results of measurements were represented by the following correlation equations

$$\lambda_{sol}(T,P,\omega) = \lambda_{H_2O}(P,T)[1 - A(100\omega + 2\times10^{-4}(100\omega)^3)] - 2\times10^{-8}PT\,100\omega \quad (1)$$

$$\lambda_{H_2O}(P,T) = 7\times10^{-9}T^3 - 1.511\times10^{-5}T^2 + 8.802\times10^{-3}T - 0.8624 + 1.6\times10^{-6}PT$$

where $\lambda_{sol}(T, P, \omega)$ is the thermal conductivity of the solution in W·m^{-1}·K^{-1}, $\lambda_{H_2O}(P, T)$ is the thermal conductivity of pure water in W·m^{-1}·K^{-1}, ω is the concentration in mass fraction, T is the temperature in K, P is the pressure in MPa, and A is the adjusting parameter. The values of coefficient A in eq 1 for H_2O + NaBr and H_2O + KBr solutions are 0.00305 and 0.0037, respectively.[19] In the limit of $\omega \to 0$, the thermal conductivity of pure water $\lambda_{H_2O}(P, T)$ is obtained from eq 1. This equation is applicable in the temperature range from (273 to 473) K, pressures from (0.1 to 100) MPa, and concentrations between (0 and 25) mass %, although some reasonable extrapolation to high concentrations is possible.

To calculate the thermal conductivity of dilute aqueous solutions, Vargaftik and Os'minin[27] used the following relationship

$$\lambda_{sol}(T) = \left[\frac{\lambda_{H_2O}(T)}{\lambda_{H_2O}(293)}\right]\lambda_{sol}(293) \quad (2)$$

where $\lambda_{sol}(293) = 598.95$ mW·m^{-1}·K^{-1} and $\lambda_{H_2O}(T)$ is the thermal conductivity of pure water. As one can see from this equation, the ratio between the thermal conductivity at 293 K and at current temperature T is collinear with that of pure water. This equation described the temperature dependence of the aqueous salt solutions within (1 to 2)% at temperatures up to 373 K.

DiGuilio,[29] DiGuilio and Teja,[30] and Bleazard et al.[31,32] were able to extend the pressure range by multiply the thermal conductivity of salt solutions λ_{sol} at atmospheric pressure (P = 0.1 MPa) by the ratio of the thermal conductivity of water at the desired pressure $\lambda_{H_2O}(P)$ to that of water at P = 0.1 MPa:

$$\lambda_{sol}(P) = \left[\frac{\lambda_{H_2O}(P)}{\lambda_{H_2O}(0.1)}\right]\lambda_{sol}(0.1) \quad (3)$$

The prediction capability of eq 3 for some aqueous solutions (H_2O + $ZnCl_2$, H_2O + $CaCl_2$, H_2O + BaI_2) was studied by Abdulagatov and Magomedov.[3,8] At pressures up to 60 MPa and concentrations of 100ω < 20 mass %, deviations between measured and predicted values of thermal conductivity are less than 1.5%. At concentrations lower than 20 mass %, the agreement is excellent (within 0.5%). For compositions above 20 mass % and pressures P > 60 MPa, the deviations are slightly higher than the experimental uncertainty (about 2%).

Chiquillo[33] proposed the following equation for the concentration dependence of the thermal conductivity of aqueous solutions:

$$\lambda_{sol} = \lambda_{H_2O}(1 + A_1x + A_2x^2) \quad (4)$$

where adjustable parameters A_i are tabulated for several electrolyte solutions (NaBr: $A_1 = -0.0311191$, $A_2 = -0.0262\times10^{-3}$; KBr: $A_1 = -0.0436497$, $A_2 = 0.2401\times10^{-3}$).

Riedel[25] proposed the following equation for the concentration dependence of aqueous salt solutions:

$$\lambda_{sol} = \lambda_{H_2O} + \sum_i \alpha_i c_i \quad (5)$$

where $\alpha(Na^+) = 0.0$, $\alpha(K^+) = -0.0065$, and $\alpha(Br^-) = -0.015$ using the ionic contribution technique.

Aseyev[22] expressed available experimental thermal conductivity data[16−18,23,24,28] from the literature for binary and ternary aqueous salt solutions by the equation

$$\lambda = \lambda_{H_2O}(1 + 100\sum_{i=1} \beta_i\omega_i) \quad (6)$$

where λ_{H_2O} is the thermal conductivity of pure water in

$W \cdot m^{-1} \cdot K^{-1}$ and ω is the concentration in mass fraction. The values of coefficients β_i in eq 6 for NaBr and KBr solutions are $\beta_1 = -0.0033144$ and $\beta_1 = -0.0042368$, respectively. This equation is valid in the temperature range from (273 to 473) K and at concentrations up to 50 mass %.

Experimental Apparatus and Procedures

Apparatus and Construction of the Thermal Conductivity Cell. The thermal conductivity of binary H_2O + NaBr and H_2O + KBr and ternary H_2O + NaBr + KBr solutions was measured by a concentric-cylinders (steady-state) technique. The experimental apparatus used in this work is the same as that previously employed for the measurement of $H_2O + Li_2SO_4$, $H_2O + Zn(NO_3)_2$, $H_2O + Ca(NO_3)_2$, $H_2O + Mg(NO_3)_2$, $Sr(NO_3)_2$, and $LiNO_3$ solutions.[11−14] The apparatus and procedures that were described previously[11−14] were used without modification. Because the apparatus has been described in detail in our previous papers,[11−14] only a brief discussion will be given here. The main part of the apparatus consisted of a high-pressure autoclave, thermostat, and thermal conductivity cell. The thermal conductivity cell consisted of two coaxial cylinders: an inner (emitting) cylinder and an outer (receiving) cylinder. The cylinders were located in a high-pressure autoclave. The deviation from concentricity was 0.002 cm or 2% of the sample layer.

The autoclave was located in the thermostat. The thermostat was a solid (massive) copper block. Temperature in the thermostat was controlled with a heater. The thermostat is supplied with a three-section heating element, PRT-10, and three chromel−alumel thermocouples were located on three different levels of the copper block. The temperature differences between various sections (levels) of the copper block were within 0.02 K of each other. Temperature was measured with a PRT and with three chromel−alumel thermocouples. Thermocouples were located on different levels of the thermostat to minimize temperature inhomogeneities. One of the junctions of a differential chromel−copel thermocouple was located in the inner cylinder and was tightly applied to the cylinder's wall. The second junction of the thermocouple was located in the shell capillary. Thermocouples were twice calibrated with a standard resistance thermometer. The difference between calibrations was 10 mK. The reading of the single thermocouples differs by ±10 mK. The measurements were started when the differences in the readings of all of the thermocouples were minimal (0.02 K).

Geometric Characteristics of the Thermal Conductivity Cell. The important dimensions of the thermal conductivity cell are o.d. of the inner cylinder $d_2 = (10.98 \pm 0.01) \times 10^{-3}$ m and i.d. of the outer cylinder $d_1 = (12.92 \pm 0.02) \times 10^{-3}$ m. The length of the measuring section of the inner cylinder (emitter) is $l = (150 \pm 0.1) \times 10^{-3}$ m. The gap between cylinders (thickness of the liquid gap) was $d = (0.97 \pm 0.03) \times 10^{-3}$ m. The choice of this gap was a compromise between decreasing convection and an accommodation effect. The optimal value of the ratio of the length l to the diameter of the inner cylinder d_2 should be $l/d_2 =$ 10 to 15.

The solution under investigation is confined in the vertical gap of the cell. Pressure in the system was created and measured with piston manometers MP-600 and MP-60 with upper limits of measurement of 600 and 60 bar, respectively. In the cell, heat was generated in the microheater that consists of an isolated (high-temperature-lacquer-covered) constantan wire of 0.1-mm diameter. A microheater was mounted inside the inner cylinder (emitter), which was closely wound around the surface of a 2-mm-diameter ceramic tube and isolated with high-temperature lacquer. The tube is tightly fitted into the heater pocket with diameter 6 mm on the inner cylinder.

Principle of Operation, Working Equation, and Corrections. With this method, the heat generated in an inner emitting cylinder is conducted radially through the narrow fluid-filled annulus to a coaxial receiving cylinder. In this method, the thermal conductivity λ of the fluid was deduced from measurements of heat Q transmitted across the solution layer, the temperature difference ΔT between the inner and outer cylinders, the thickness of the solution layer d, the and effective length l of the measuring part of the cylinder (effective length of the cylinders).

After taking into account all corrections, we can write the final working equation for the thermal conductivity as

$$\lambda = A\frac{Q_{\text{meas}} - Q_{\text{los}}}{\Delta T_{\text{meas}} - \Delta T_{\text{corr}}} \tag{7}$$

where $A = \ln(d_2/d_1)/2\pi l$ is the geometric constant that can be determined with geometrical characteristics of the experimental cell; Q_{meas} is the amount of heat released by the calorimetric microheater; Q_{los} is the amount of heat lost through the ends of the measuring cell (end effect); $\Delta T_{\text{corr}} = \Delta T_{\text{cl}} + \Delta T_{\text{lac}}$; ΔT_{cl} and ΔT_{lac} are the temperature differences in the cylinder walls and lacquer coat, respectively; and ΔT_{meas} is the temperature difference measured with differential thermocouples. The values of A can be also determined by means of a calibration technique using thermal conductivity data for the reference fluid (pure water, IAPWS[34]). The values of the cell constant determined with both geometrical characteristics of the experimental cell and calibration techniques (pure water at temperature 293.15 K) are 0.1727 m^{-1} and 0.1752 m^{-1}, respectively. In this work, we used the value of A as a function of temperature derived using the calibration procedure with pure water (IAPWS[34]). The geometrical constant A changes by 12% over the temperature range from (293.15 to 750.15) K. The change in the cell size due to pressure was considered negligible because of the low volume compressibility of stainless steel (1X18H9T).

Because of the large emitter size and the small fluid volume surrounding the emitter, no effect of accommodation was to be expected. The calibration of the cell was made at a pressure of 60 MPa to avoid corrections due to the accommodation effect.

It is difficult to estimate the values of Q_{los} and ΔT_{corr} by calculation. In this work, the values of Q_{los} and ΔT_{corr} were estimated by measuring standard liquids (water) with well-known thermal conductivity (IAPWS[34] standard). Calibration was made with pure water at 10 selected temperatures between (293.15 and 713.15) K and at 3 selected pressures between (0.1 and 60) MPa. The amount of heat flow Q and the temperature difference ΔT were 13.06 W and 3.5 K, respectively. The estimated value of Q_{los} is about 0.05 W. This value is negligible (0.38%) by comparison with the heat transfer by conduction $Q = 13.06$ W.

Convection Heat Transfer. Convection heat transfer increases with increasing values of the Rayleigh number (Ra). To reduce the values of Ra, a small gap distance between cylinders $d = (0.97 \pm 0.03) \times 10^{-3}$ m was used. This makes it possible to minimize the risk of convection. Convection could develop when the Ra exceeds a certain critical value Ra_c, which for vertical coaxial cylinders is about 1000 (Gershuni[35]). Therefore, $Ra > 1000$ was considered to be a criterion for the beginning of convection.

Table 2. Comparison between Experimental Thermal Conductivity Data and Values Calculated with IAPWS[34] Standard for Pure Water (AAD = 0.51%)

	P/MPa = 1.0		P/MPa = 10		P/MPa = 40	
T/K	this work	λ/W·m^{-1}·K^{-1} IAPWS[34]	this work	λ/W·m^{-1}·K^{-1} IAPWS[34]	this work	λ/W·m^{-1}·K^{-1} IAPWS[34]
290.6	0.592	0.594	0.602	0.599	0.613	0.613
329.7	0.649	0.651	0.655	0.656	0.665	0.669
367.1	0.679	0.677	0.684	0.682	0.697	0.698
395.1	0.683	0.684	0.692	0.689	0.709	0.707
440.7			0.683	0.684	0.703	0.705
484.2			0.660	0.663	0.684	0.689
514.2			0.638	0.638	0.662	0.669
549.8			0.587	0.592	0.628	0.634
575.4			0.540	0.546	0.594	0.601

In the range of the present experiments, the values of Ra were always less than 500, and Q_{con} are estimated to be negligibly small. The absence of convection can be verified experimentally by measuring the thermal conductivity with different temperature differences ΔT across the measurement gap and a different power Q transferred from the inner to outer cylinder. The measured thermal conductivity data were indeed independent of the applied temperature differences ΔT and power Q transferred from the inner to outer cylinder.

Heat Transfer by Radiation. Any conductive heat transfer must be accompanied by simultaneous radiative transfer. The correction depends on whether the fluid absorbs radiation. If the fluid is entirely transparent, then the conductive and radiative heat fluxes are additive and independent and the simple correction given by Healy et al.[36] is adequate and usually negligible. When the fluid absorbs and re-emits radiation (partially transparent), the problem is more complicated because then the radiative and conductive fluxes are coupled. The inner and outer cylinders were perfectly polished with powder of successively smaller grain size (320 nm); their emissivity (ϵ = 0.32) was small, and the heat flux arising from radiation Q_{rad} is negligible by comparison with the heat transfer by conduction in the temperature range of our experiment. To minimize the heat transfer by radiation, a solid material (stainless steel 1X18H9T) of low emissivity was used for the cylinders, and thin layers of fluid (from 0.97 mm) were used. In this way, heat transport by radiation can be strongly reduced compared to the heat transport by conduction. The correction for absorption is therefore small for pure water and for aqueous solutions in the temperature range up to 600 K, and we assumed that it was negligible. Its influence on the uncertainty of the thermal conductivity is relatively small.

The emissivity of the walls was small, and Q_{rad} is negligible (~0.164 W) by comparison with the heat transfer (13.06 W) by conduction in the temperature range of our experiment.

Assessment of Uncertainties. The uncertainty analysis was carried out similarly to that in previous work (Abdulagatov et al.[11]). Measurement uncertainties were associated with uncertainties that exist in measured quantities contained in working eq 7 used to compute the thermal conductivity from experimental data. The thermal conductivity was obtained from the measured quantities A, Q, T, ΔT, P, and ω. The accuracy of the thermal conductivity measurements was assessed by analyzing the sensitivity of eq 7 to the experimental uncertainties of the measured quantities.

Because the uncertainties of the measured values d_1, d_2, and l are 0.15%, 0.09%, and 0.07%, respectively, the corresponding uncertainty of A is 0.5%. The experimental uncertainty of the concentration is estimated to be 0.02%. The uncertainties of temperature and pressure measurements are θ_T = 0.02 K and θ_P = 0.03 MPa at a pressure of 60 MPa. The corresponding uncertainty of the thermal conductivity measurement related to the uncertainties of temperature and pressure measurements is estimated to be less than 0.006%. The uncertainty of the heat flow Q measurement is about 0.1%. To make sure the cell was at equilibrium, the measurements were started 10 h after the time when the thermostat temperature reached the prescribed temperature. About five to six measurements are carried out at one state, and the average value of the thermal conductivity is calculated. The reproducibility (scattering of the different measurements) of the measurements is about 0.5%. From the uncertainty of the measured quantities and the corrections mentioned above, the total maximum relative uncertainty $\delta\lambda/\lambda$ in measuring the thermal conductivity was 2%.

Performance Tests. To check and confirm the accuracy of the method and the procedure of the measurements, thermal conductivity data were taken for pure water in the temperature range from (290.6 to 575.4) K at pressures up to 40 MPa. Table 2 provides a detailed comparison of present test measurement results for pure water with the reference data for water (IAPWS[34]). Table 2 demonstrates that the agreement between test measurements for pure water and IAPWS[34] calculations is excellent; deviation statistics are AAD = 0.51, bias = −0.34, std dev = 0.55, std err = 0.12, and max dev = 1.18%. Excellent agreement is also found between the present thermal conductivity results for pure water and the data reported by other authors (AAD within 0.2 to 1.2%) and reference data reported by Ramires et al.[37] (AAD = 0.3%). This excellent agreement for test measurements confirms the reliability and accuracy of the present measurements for binary (H_2O + NaBr and H_2O + KBr) and ternary (H_2O + NaBr + KBr) solutions and corrects the operation of the instrument.

The solutions at the desired composition were prepared by mass. The composition was checked by a comparison of the density of solutions at 293.15 K and 0.1 MPa with reference data.

Results and Discussion

Measurements of the thermal conductivity for the binary aqueous NaBr solutions were performed near the saturation curve (0.1 to 2 MPa) and along two isobars (10 and 40) MPa between (294 and 577) K for four compositions, namely, (10, 20, 30, and 38) mass %. For binary aqueous KBr solutions, measurements were made at the same isobars for three compositions of (10, 20, and 30) mass % between (294 and 576) K. For the three ternary solutions (H_2O + 10% NaBr + 5% KBr, H_2O + 10% NaBr + 10%

Table 3. Experimental Thermal Conductivities (λ/W·m^{-1}·K^{-1}), Pressures, Temperatures, and Concentrations of Binary H_2O + NaBr Solutions

	100ω/mass % = 10				100ω/mass % = 20		
T/K	*P*/MPa = 0.1 to 2	*P*/MPa = 10	*P*/MPa = 40	*T*/K	*P*/MPa = 0.1 to 2	*P*/MPa = 10	*P*/MPa = 40
294.3	0.580	0.586	0.596	296.0	0.560	0.565	0.575
321.7	0.618	0.624	0.635	319.9	0.595	0.599	0.609
354.2	0.648	0.653	0.664	350.2	0.624	0.628	0.639
378.6	0.659	0.663	0.674	377.9	0.637	0.642	0.653
399.2	0.664	0.669	0.679	396.5	0.643	0.648	0.659
427.5	0.664	0.671	0.682	429.2	0.643	0.649	0.659
453.7	0.652	0.659	0.672	450.6	0.632	0.638	0.652
486.2		0.639	0.660	483.2		0.618	0.634
515.3		0.611	0.634	519.4		0.583	0.601
542.7		0.576	0.604	547.6		0.546	0.571
577.3		0.525	0.566	576.2		0.504	0.535
	100ω/mass % = 30				100ω/mass % = 38		
T/K	*P*/MPa = 0.1 to 2	*P*/MPa = 10	*P*/MPa = 40	*T*/K	*P*/MPa = 0.1−2	*P*/MPa = 10	*P*/MPa = 40
297.2	0.537	0.541	0.550	294.7	0.504	0.512	0.525
323.9	0.573	0.578	0.587	319.6	0.531	0.536	0.549
357.7	0.601	0.608	0.617	347.2	0.560	0.565	0.578
380.2	0.610	0.617	0.627	374.5	0.580	0.589	0.603
401.0	0.615	0.623	0.633	398.7	0.585	0.593	0.609
426.4	0.614	0.624	0.637	424.5	0.585	0.593	0.609
455.0	0.600	0.608	0.621	456.7	0.572	0.583	0.600
				483.2		0.569	0.590
				515.7		0.535	0.565
				541.3		0.504	0.539
				576.5		0.454	0.494

Table 4. Experimental Thermal Conductivities, Pressures, Temperatures, and Concentrations of Binary H_2O + KBr Solutions

	100ω/mass % = 10				100ω/mass % = 20		
T/K	*P*/MPa = 0.1 to 2	*P*/MPa = 10	*P*/MPa = 40	*T*/K	*P*/MPa = 0.1 to 2	*P*/MPa = 10	*P*/MPa = 40
294.7	0.578	0.582	0.592	296.8	0.553	0.557	0.565
320.9	0.612	0.617	0.628	325.4	0.589	0.595	0.602
354.8	0.644	0.650	0.662	351.2	0.616	0.620	0.629
381.3	0.661	0.669	0.682	387.6	0.634	0.638	0.647
403.2	0.661	0.667	0.683	406.2	0.632	0.638	0.648
425.9	0.657	0.662	0.681	431.2	0.628	0.634	0.646
457.6	0.643	0.650	0.665	456.9	0.616	0.623	0.635
488.2		0.628	0.650	481.3		0.609	0.623
519.3		0.598	0.622	520.6		0.575	0.592
543.2		0.569	0.597	547.6		0.539	0.564
571.9		0.522	0.550	571.3		0.501	0.534

	100ω/mass % = 30		
T/K	*P*/MPa = 0.1 to 2	*P*/MPa = 10	*P*/MPa = 40
295.7	0.521	0.525	0.532
321.4	0.554	0.559	0.569
357.6	0.588	0.591	0.601
384.2	0.601	0.605	0.616
409.6	0.600	0.606	0.618
427.2	0.598	0.604	0.616
463.1	0.582	0.586	0.599
494.2		0.564	0.579
516.3		0.542	0.562
539.7		0.511	0.538
575.6		0.455	0.496

KBr, and H_2O + 10% NaBr + 20% KBr), measurements were made in the same temperature and pressure ranges. The experimental temperature, pressure, composition, and thermal conductivity values are presented in Tables 3 to 5. The values of $T_{ave} = T_1 + 0.5\Delta T$, where T_1 is the temperature of the outer cylinder and ΔT is the temperature difference across the measurement gap, were accepted as experimental temperatures. Some selected experimental results are shown in Figures 1a and b to 5a and b in the $\lambda - T$, $\lambda - P$, and $\lambda - \omega$ spaces together with values reported by other authors and calculated from various correlation equations from the literature. The thermal conductivity of solutions was measured as a function of temperature at constant pressure for various compositions. In Figures 1a and b and 2a and b, the temperature dependence data of the measured values of thermal conductivity for H_2O + NaBr and H_2O + KBr solutions near the saturation curve (0.1 to 2 MPa) and along isobar 40 MPa and a composition of 10 mass % of salt are presented. As one can see, on each isopleth−isobar $\lambda - T$ curve, the thermal conductivity of solutions increases with temperature, passes through a maximum between (400 and 427) K for H_2O + NaBr and between (403 and 410) K for H_2O + KBr depending on pressure and concentration, and decreases at higher temperatures such as that for pure water. For pure water, this maximum occurs at temperatures between (409 and 421)

Table 5. Experimental Thermal Conductivities, Pressures, Temperatures, and Concentrations of Ternary H_2O + NaBr + KBr Solutions

	100ω/mass % = 10NaBr+5KBr				100ω/mass % = 10NaBr + 10KBr				100ω/mass % = 10NaBr + 20KBr		
T/K	P/MPa = 0.1 to 2	P/MPa = 10	P/MPa = 40	T/K	P/MPa = 0.1 to 2	P/MPa = 10	P/MPa = 40	T/K	P/MPa = 0.1 to 2	P/MPa = 10	P/MPa = 40
296.8	0.570	0.575	0.585	295.3	0.556	0.563	0.570	297.4	0.540	0.545	0.556
325.6	0.611	0.616	0.624	318.4	0.587	0.593	0.605	322.9	0.575	0.580	0.589
347.7	0.630	0.635	0.647	349.3	0.618	0.625	0.634	354.1	0.602	0.607	0.618
382.1	0.654	0.660	0.666	378.8	0.635	0.638	0.647	377.8	0.615	0.621	0.629
411.9	0.651	0.657	0.665	404.7	0.637	0.641	0.653	407.3	0.620	0.626	0.636
440.4		0.650	0.661	438.7	0.630	0.636	0.650	429.5	0.617	0.623	0.634
472.9		0.635	0.645	476.1		0.615	0.630	454.6	0.604	0.610	0.622
507.9		0.602	0.620	505.3		0.593	0.608	486.8	0.586	0.593	0.604
539.6		0.560	0.590	542.8		0.547	0.566	509.1	0.569	0.575	0.587
577.3		0.507	0.535	568.3		0.507	0.527	538.0	0.533	0.540	0.558
								573.9	0.472	0.480	0.516

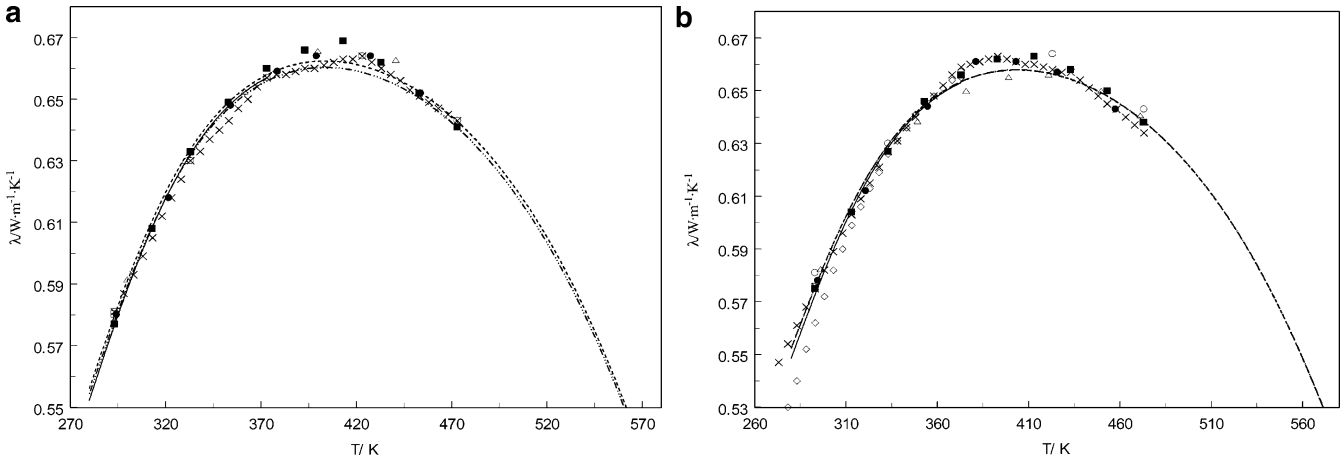

Figure 1. Measured values of thermal conductivity of H_2O + NaBr (a) and H_2O + KBr (b) as a function of temperature near the saturated curve (0.1 to 2) MPa together with data and correlations reported by other authors in the literature. H_2O + NaBr (a): ●, this work; ○, El'daraov;[17] ■, Magomedov;[19] □, Riedel;[25] Δ, Rastorguev et al.;[16] ×, Aseyev;[22] —, Chiquillo[33] (eq 4); – – –, Magomedov[19] (eq 1); – ··· – ··· – ···, Vargaftik and Os'minin.[27] H_2O + KBr (b): ●, this work; ○, El'daraov;[17] ■, Abdulagatov and Magomedov;[10] □, Riedel;[25] Δ, Safronov et al.;[20,21] ×, Aseyev;[22] —, Chiquillo[33] (eq 4); – – –, Abdulagatov and Magomedov[10] (eq 1); – ··· – ··· – ···, Vargaftik and Os'minin.[27]

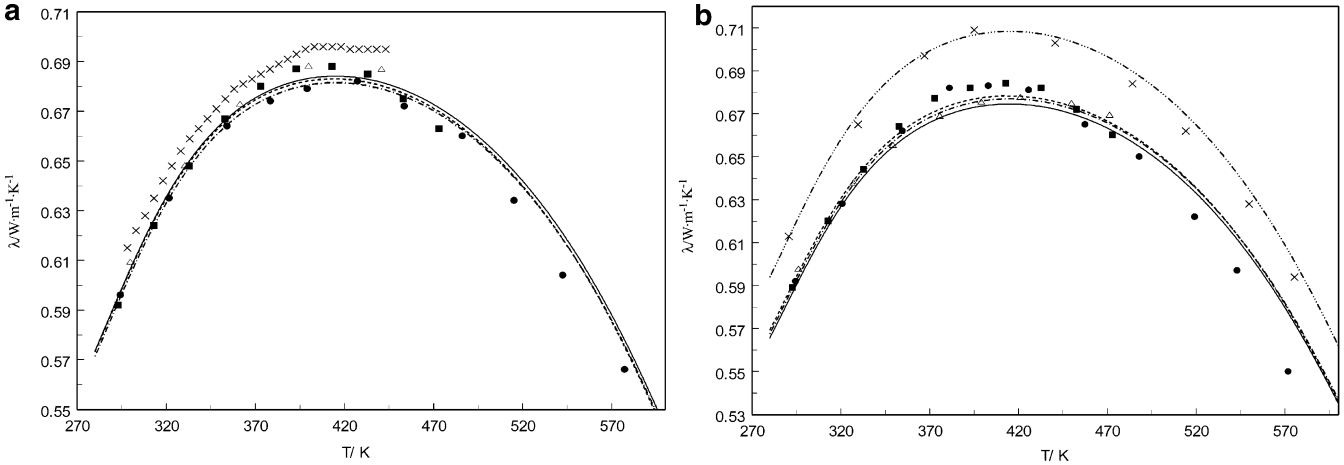

Figure 2. Measured values of thermal conductivity of H_2O + NaBr (a) and H_2O + KBr (b) as a function of temperature along the selected isobar of 40 MPa and concentration of 10 mass % together with values reported by other authors in the literature and calculated with various correlation and prediction equations. H_2O + NaBr (a): ●, this work; ■, Magomedov;[19] Δ, Rastorguev et al.;[16] ×, Aseyev;[22] —, Chiquillo[33] (eq 4); – – –, Magomedov[19] (eq 1); – ··· – ··· – ···, Vargaftik and Os'minin.[27] H_2O + KBr (b): ●, this work; ■, Abdulagatov and Magomedov;[10] Δ, Safronov et al.;[20,21] —, Chiquillo[33] (eq 4); – – –, Abdulagatov and Magomedov[10] (eq 1); – ··· – ··· – ···, Vargaftik and Os'minin.[27]

K as pressure changes from (20 to 60) MPa. Therefore, adding salt slightly shifts the thermal conductivity maximum to high temperatures. Abdulagatov and Magomedov[3,6–10] studied the pressure and composition dependence of the thermal conductivity maximum for aqueous salt solutions. The values of temperature for which $(\partial\lambda/\partial T)_{P,\omega} = 0$, where the isobar–isopleth maximum of the thermal conductivity occurred, can be calculate using eq 1 as

$$T_m(P, \omega) = \frac{a}{2} - \left(\frac{a^2}{4} - b\right)^{1/2} \quad (8)$$

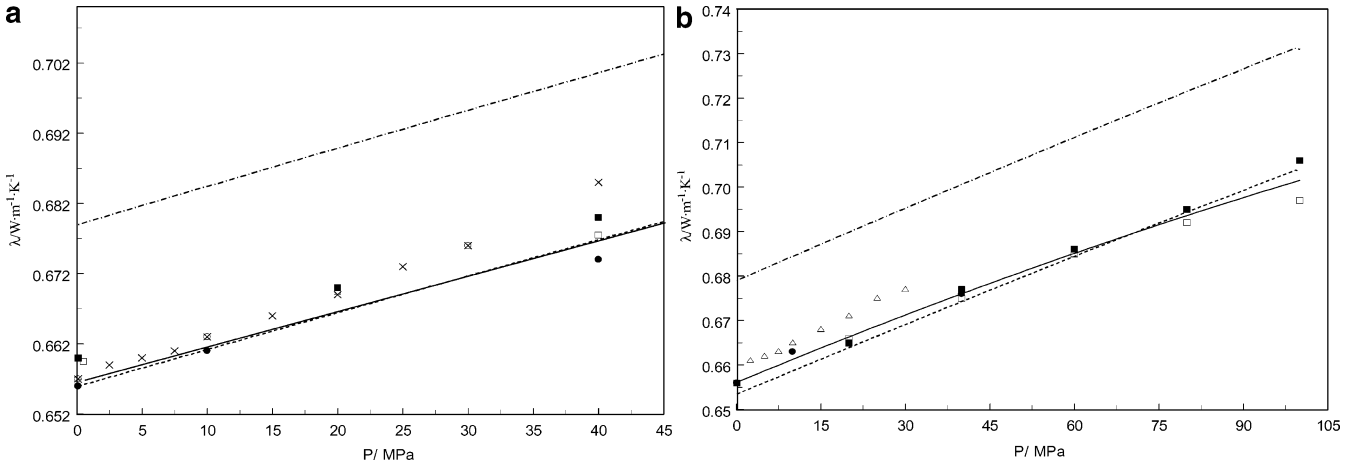

Figure 3. Measured values of thermal conductivity of H_2O + NaBr (a) and H_2O + KBr (b) as a function of pressure along the selected isotherm of 373.15 K and concentration of 10 mass % together with values calculated with correlation equations and reported data from the literature. H_2O + NaBr (a): ●, this work; ○, El'darov;[17] ■, Magomedov;[19] □, Rastorguev et al.;[16] ×, Aseyev;[22] —, Magomedov[19] (eq 1); – – –, DiGuilio et al.[29,30] and Bleazard et al.[31,32] (eq 3); – · – · –, pure water (IAPWS[34]). H_2O + KBr (b): ●, this work; ○, El'darov;[17] ■, Abdulagatov and Magomedov;[10] □, Safronov et al.;[20,21] Δ, Abdullaev et al.;[18] —, Abdulagatov and Magomedov[10] (eq 1); – – –, DiGuilio et al.[29,30] and Bleazard et al.[31,32] (eq 3); – · – · –, pure water (IAPWS[34]).

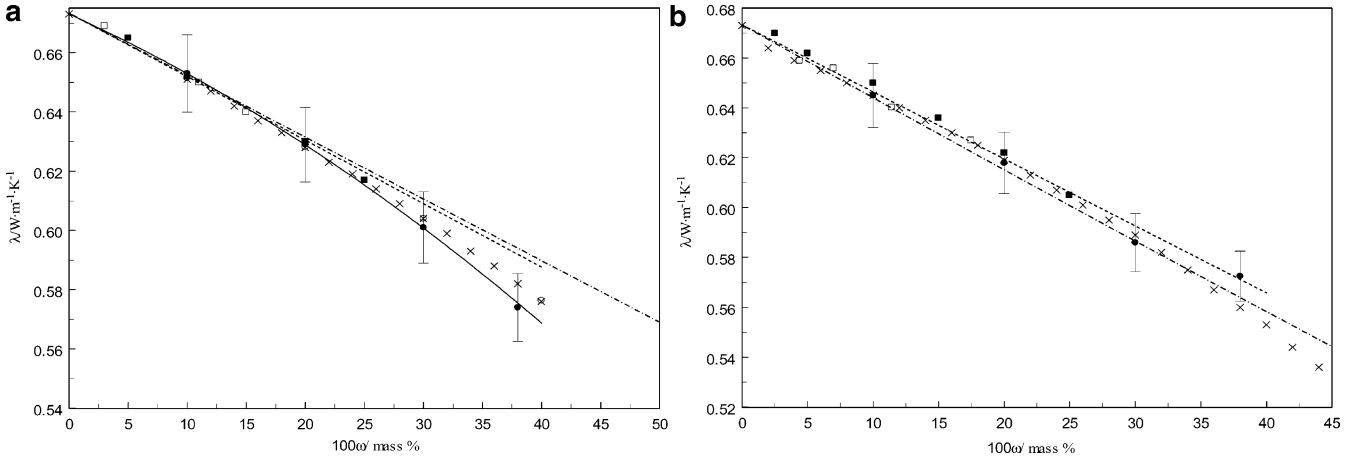

Figure 4. Measured values of thermal conductivity of H_2O + NaBr (a) and H_2O + KBr (b) as a function of composition at a selected temperature of 453.15 K near the saturated curve together with values calculated from various correlations and the data reported in the literature. H_2O + NaBr (a): ●, this work; ○, El'darov;[17] ■, Magomedov;[19] □, Rastorguev et al.;[16] ×, Aseyev;[22] —, Magomedov[19] (eq 1); – – –, Riedel;[25] – · – · – ·, Chiquillo[33] (eq 4). H_2O + KBr (b): ●, this work; ○, El'darov;[17] ■, Abdulagatov and Magomedov;[10] □, Safronov et al.;[20,21] ×, Aseyev;[22] —, Abdulagatov and Magomedov[10] (eq 1); – – –, Riedel;[25] – · – · – ·, Chiquillo[33] (eq 4).

where

$$b = \frac{4.191429 \times 10^5 + P[76.19 - 76.19A(\omega - 2 \times 10^{-4}\omega^3) - 0.95238\omega]}{1 - A(\omega - 2 \times 10^{-4}\omega^3)}$$

and

$$a = 1439.0476.$$

The maximum temperatures of the thermal conductivity of H_2O + NaBr calculated with eq 8 at pressures of (0.1 and 40) MPa and at composition of 10 mass % are (405.57 and 409.82) K, respectively. Pure water shows the maximum thermal conductivity almost at the same temperatures for the same pressures.

Figure 3a and b shows the results of the thermal conductivity measurements for H_2O + NaBr and H_2O + KBr solutions as a function of pressure for a selected composition (10 mass %) and temperature (373.15 K). Along each isopleth−isotherm, the thermal conductivity increases almost linearly as the pressure increase at pressures up to 40 MPa and is not parallel to those of pure water, especially at high concentrations and high temperatures (Figure 3a and b). The magnitude of the increase at a pressure of 40 MPa and a temperature of 373 K is about (2 to 2.5)%. The slope of the water isotherms ($\lambda - P$) is higher than the slopes of the solutions isotherms, especially at high concentrations. At high pressures (40 MPa) and high concentrations (20 mass %), the absolute values of the thermal conductivity of water are higher (about 8−12%) than those of solutions. At low pressures (10 MPa) and low concentrations (10 mass %), differences between pure water and solution thermal conductivities is about (5 to 8)%.

The composition dependences of the measured thermal conductivities for H_2O + NaBr and H_2O + KBr solutions for the selected isotherm 453.15 K and at pressures of (0.1 to 2) MPa (near the saturated curve) are shown in Figure 4a and b together with data reported by other authors. The thermal conductivity of the solution monotonically decreases with composition. As one can see from Figure 4a and b, the composition dependence of the thermal conductivity exhibits a small curvature at high compositions ($100\omega > 20$ mass %). Extrapolation of the high-composition

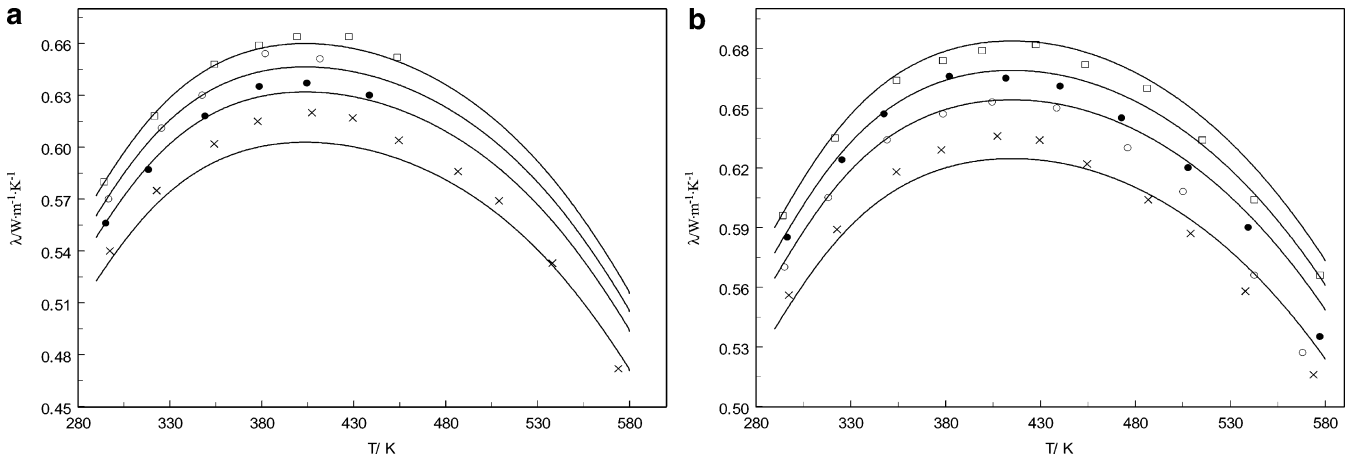

Figure 5. Measured values of thermal conductivity of ternary H_2O + NaBr + KBr solutions as a function of temperature for various compositions of KBr together with values for binary H_2O + NaBr and H_2O + KBr solutions. (a) $P = 0.1-2$ MPa: □, H_2O + 10% NaBr + 0% KBr; ●, H_2O + 10% NaBr + 5% KBr; ○, H_2O + 10% NaBr + 10% KBr; H_2O + 10% NaBr + 20% KBr. (b) $P = 40$ MPa: □, H_2O + 10% NaBr + 0% KBr; ●, H_2O + 10% NaBr + 5% KBr; ○, H_2O + 10% NaBr + 10% KBr; H_2O + 10% NaBr + 20% KBr. —, Aseyev[22] (calculated with eq 6).

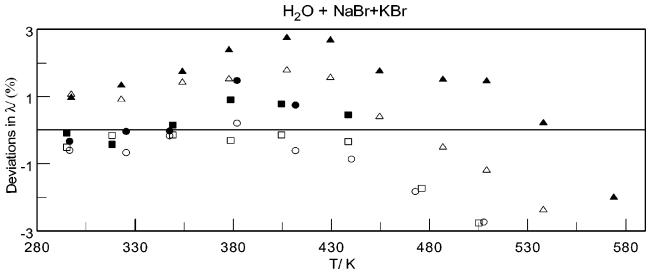

Figure 6. Percentage thermal conductivity deviations, $\delta\lambda = 100\text{-}(\lambda_{exp} - \lambda_{cal})/\lambda_{cal}$, of the experimental thermal conductivities for ternary H_2O + 10% NaBr + KBr solutions from the values calculated with correlation eq 6. $P = 0.1-2$ MPa: ●, 5 mass %; ■, 10 mass %; ▲, 20 mass %. $P = 40$ MPa: ○, 5 mass %; □, 10 mass %; Δ, 20 mass %.

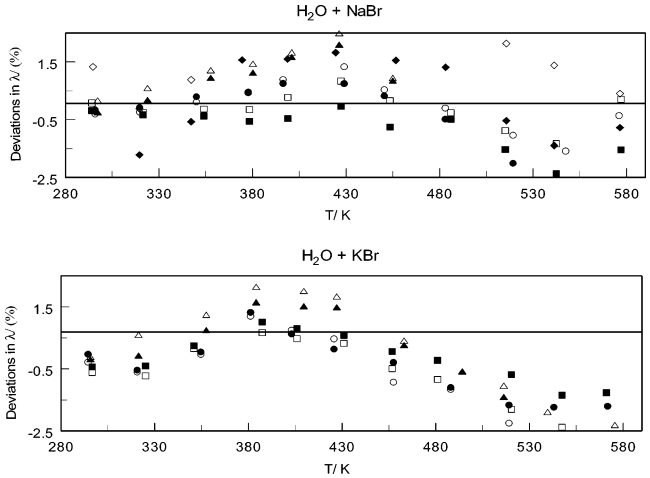

Figure 7. Percentage thermal conductivity deviations, $\delta\lambda = 100\text{-}(\lambda_{exp} - \lambda_{cal})/\lambda_{cal}$, of the experimental thermal conductivities for H_2O + NaBr and H_2O + KBr solutions from the values calculated with eq 1. H_2O + NaBr: ○, 10 MPa and 20 mass %; ●, 40 MPa and 20 mass %; □, 10 MPa and 10 mass %; ■, 40 MPa and 10 mass %; Δ, 10 MPa and 30 mass %; ▲, 40 MPa and 30 mass %; ◆, 40 MPa and 38 mass %; ◇, 10 MPa and 38 mass %. H_2O + KBr: ○, 40 MPa and 10 mass %; ●, 10 MPa and 10 mass %; □, 40 MPa and 20 mass %; ■, 10 MPa and 20 mass %; Δ, 40 MPa and 30 mass %; ▲, 10 MPa and 30 mass %.

measurements to zero concentration ($\omega \rightarrow 0$) gives values in good agreement with the data for pure water (Figure 4a and b) calculated with the IAPWS[34] formulation.

Figure 5a and b shows the temperature dependences of the thermal conductivity of three ternary solutions H_2O + 10% NaBr + 5% KBr, H_2O + 10% NaBr + 10% KBr, and H_2O + 10% NaBr + 20% KBr together with values for binary solution H_2O + 10% NaBr along isobar 40 MPa and near the saturation curve (0.1 to 2 MPa). This Figure also contains the values of thermal conductivity for ternary solutions calculated with correlation eq 6 (Aseyev[22]). The agreement between experimental and calculated values for the ternary H_2O + 10% NaBr + KBr solutions is within 0.8% at temperatures up to 473 K where eq 6 is valid. Above 473 K (extrapolated to high temperatures), the deviations increased to (3 to 7)%. A deviation plot is shown in Figure 6. The deviation statistics are AAD = 0.84, bias = 0.23, std dev = 1.02, std err = 0.16, max dev = 2.7, and $N = 50$. Excellent agreement within 0.5% between measured and calculated values of the thermal conductivity is found at low concentrations ($100\omega < 20$ mass % KBr). At a concentration of 20 mass %, calculated values are systematically lower (about 0.8% at $T < 473$ K) than measured values. Figure 5a and b show that adding 5% and 20% of the third component (KBr) in the binary H_2O + 10% NaBr solution decreasing the thermal conductivity of the ternary solution by 2% and 5%, respectively.

Figures 1a and b to 4a and b demonstrated the direct comparison of the present measurements of thermal conductivity for H_2O + NaBr and H_2O + KBr solutions with the data reported by other authors and values calculated with various correlation equations from the literature. These Figures contain the values of thermal conductivity for H_2O + NaBr and H_2O + KBr measured by various authors from the literature (Table 1) and calculated with correlation eqs 1 to 6 together with the present results. The deviation plots between the present data and values calculated with correlation eq 1 are given in Figure 7. The deviation statistics of the comparisons between the present thermal conductivity data and the values calculated with correlation eq 1 for H_2O + NaBr and H_2O + KBr solutions are given in Table 6. For all of the data, the AAD values are 0.83% and 0.92%, respectively, for H_2O + NaBr and H_2O + KBr solutions. Only the extrapolation of eq 1 to high temperatures (above 473.15 K) and to high compositions (above 25 mass %) represents the thermal conductivity of H_2O + NaBr and H_2O + KBr solutions with an accuracy

Table 6. Deviation Statistics for H_2O + NaBr and H_2O + KBr Solutions

deviation	H_2O + NaBr	H_2O + KBr
AAD	0.83	0.92
bias	0.17	−0.16
std dev	1.04	1.14
std err	0.12	0.15
max dev	2.47	2.4
N	80	63

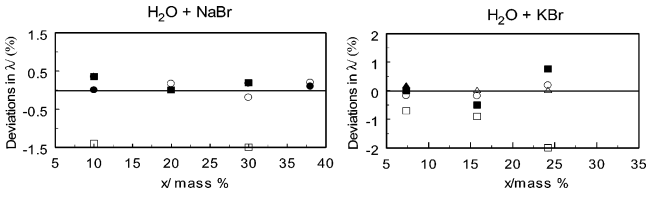

Figure 8. Percentage thermal conductivity deviations, $\delta\lambda = 100\text{-}(\lambda_{exp} - \lambda_{cal})/\lambda_{cal}$, of the experimental thermal conductivities for H_2O + NaBr and H_2O + KBr solutions from the values reported by other authors at a temperature of 293.15 K and atmospheric pressure. H_2O + NaBr: ●, El'darov;[17] □, Kapustinskii and Ruzavin;[26] ○, Riedel;[25] ■, Magomedov.[19] H_2O + KBr: ○, Riedel;[25] ▲, Rastorguev et al.;[16] □, Kapustinskii and Ruzavin;[26] Δ, Vargaftik and Os'minin;[27] ■, Abdulagatov and Magomedov.[10]

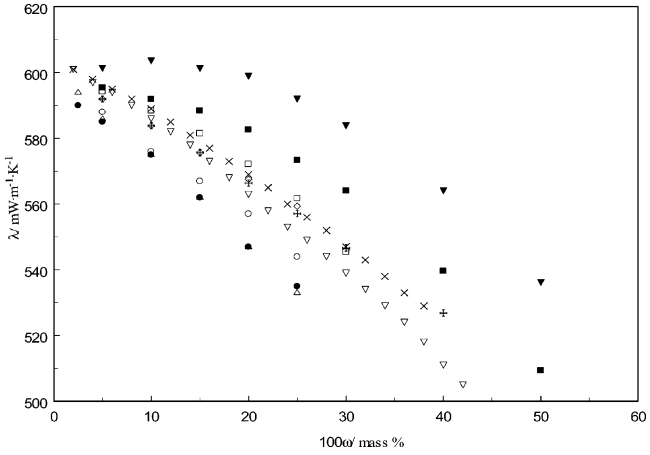

Figure 9. Thermal conductivity of a series of aqueous solutions as a function of concentration at a pressure of 0.1 MPa and a temperature 293.15 K. ●, KBr (this work); ○, KCl (Abdulagatov and Magomedov[2]); Δ, KI (Abdulagatov and Magomedov[10]); □, KF (Riedel[25]); +, KNO_2 (Riedel[25]); ▼, KOH (Riedel[25]); ■, K_2CO_3 (Riedel[25]); ◊, $K_4Fe(CN)_6$ (Riedel[25]); × , K_2CrO_4 (Aseyev[22]); ∇, K_3PO_4 (Aseyev[23]).

that slightly exceeds the experimental uncertainty (2%). Excellent agreement (within 0.2 to 0.5%) is found between the present data and values reported by Riedel[25] and Vargaftik and Os'minin[27] (deviation plot, Figure 8). Figure

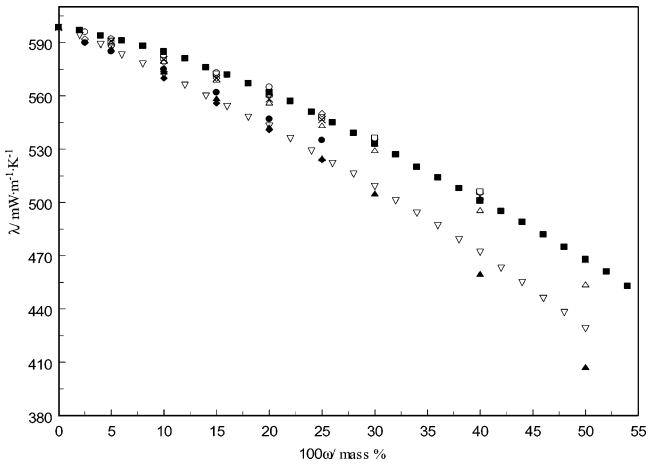

Figure 10. Thermal conductivity of a series of aqueous solutions reported by various authors as a function of composition at a selected temperature of 293.15 K and a pressure of 0.1 MPa. ●, KBr (this work); ○, $CdBr_2$ (Abdulagatov and Magomedov[5]); Δ, $CaBr_2$ (Abdulagatov and Magomedov[15]); □, $SrBr_2$ (Abdulagatov and Magomedov[9]); × , NaBr (this work); ◆, LiBr (Abdulagatov and Magomedov[4]); ▲, $MgBr_2$ (Riedel[25]); ◊, $BaBr_2$ (Magomedov[19]); ■, $CoBr_2$ (Aseyev[22]); ∇, CsBr (Aseyev[22]).

3b demonstrates that the data reported by Abdullaev et al.[18] for H_2O + KBr solutions at 373.15 K and 10 mass % is systematically higher (by 1.0 to 1.5%) than the present data and the other data sets. Figure 4a and b also illustrates the good consistency of the concentration dependence of the thermal conductivity for H_2O + NaBr and H_2O + KBr solutions measured in the present work and reported by other authors.[10,16−28]

The excellent agreement within (0.3 to 0.6)% is observed between the present thermal conductivity results for H_2O + NaBr and H_2O + KBr solutions and the values predicted with correlation eqs 2 to 4 (Figures 1 to 3a and b).

Figures 9 and 10 include the thermal conductivity data of a series of aqueous solutions with the same cation (K^+) and various anions (Br^-, Cl^-, I^-, F^-, NO_2^-, OH^-, CO_3^-, CrO_4^-, and PO_4^-, Figure 9) and the same anion (Br^-) and various cations (K^+, Na^+, Li^+, Ca^+, Mg^+, Ba^+, Co^+, Sr^+, Cd^+, and Cs^+ , Figure 10) as a function of concentration. These Figures demonstrate the effect of various anions and cations on the values and behavior of the thermal conductivity of salt solutions. As one can see from Figure 9, the H_2O + KBr and H_2O + KI solutions had the lowest values of thermal conductivity among aqueous solutions (KCl, KBr, KF, KNO_2, K_2CO_3, $K_4Fe(CN)_6$, K_2CrO_4, and K_3PO_4) at the same thermodynamic (*P, T, ω*) conditions, whereas the thermal conductivity of the H_2O + KOH solution had the highest values. Figure 10 demonstrates the concentra-

Table 7. Parameters a_{ijk} of Equation 9

H_2O + NaBr

	i = 0		*i* = 1		*i* = 2	
k	*j* = 0	*j* = 1	*j* = 0	*j* = 1	*j* = 0	*j* = 1
0	0.5714×10^{0}	5.0420×10^{-4}	-1.6139×10^{-2}	-3.267×10^{-5}		
1	1.6098×10^{-3}	-3.6809×10^{-6}	2.9323×10^{-7}	2.993×10^{-7}		
2	-6.0180×10^{-6}	3.6510×10^{-8}	1.3233×10^{-7}	-1.331×10^{-8}	-1.448×10^{-8}	1.687×10^{-9}

H_2O + KBr

	i = 0		*i* = 1		*i* = 2	
k	*j* = 0	*j* = 1	*j* = 0	*j* = 1	*j* = 0	*j* = 1
0	0.5639×10^{0}	4.9280×10^{-4}	-2.1711×10^{-2}	2.5987×10^{-5}		
1	-1.5765×10^{-3}	2.1105×10^{-6}	1.0472×10^{-5}	-1.7914×10^{-6}		
2	-6.0186×10^{-6}	8.3640×10^{-8}	3.0810×10^{-7}	-5.3400×10^{-8}	-7.6950×10^{-8}	1.0053×10^{-8}

tion dependence of the thermal conductivity of alkali bromides (NaBr, KBr, $CdBr_2$, LiBr, $SrBr_2$, $CaBr_2$, $CoBr_2$, CsBr, and $MgBr_2$). Among these solutions, H_2O + NaBr and H_2O + KBr have intermediate values of thermal conductivity.

The results of the (λ, P, t, m) measurements for H_2O + NaBr and H_2O + KBr solutions were represented by the equation

$$\lambda/\mathrm{W\cdot m^{-1}\cdot K^{-1}} = \sum_{i=0}^{1}\sum_{j=0}^{1}\sum_{k=0}^{2} a_{ijk} m^i P^j t^k \qquad (9)$$

where λ is the thermal conductivity of the solution, t is the temperature in °C, P is the pressure in MPa, and m is the composition in molality. At high concentrations (>1 m), nonlinear terms for the composition dependence in eq 9 have to be included. Equation 9 describes the thermal conductivity of H_2O + NaBr and H_2O + KBr solutions with an accuracy that does not exceed the experimental uncertainty. The average absolute deviation between values measured and calculated with eq 9 is 1.5%. The coefficients of eq 9 have been determined using fitting procedure. The derived values of coefficients a_{ij}, b_{ij}, $c_{i,j}$, and d_{ij} in eq 9 for H_2O + NaBr and H_2O + KBr solutions are given in Table 7. Equation 9 is valid in the temperature range from (293 to 580) K, at pressures up to 40 MPa, and for composition up to 4 m.

Conclusions

The thermal conductivity of four aqueous NaBr solutions of (10, 20, 30, and 38) mass %, three aqueous KBr solutions of (10, 20, and 30) mass %, and three aqueous NaBr + KBr solutions (10% NaBr + 5% KBr, 10% NaBr + 10% KBr, and 10% NaBr + 20% KBr) has been measured with a coaxial-cylinder (steady-state) technique. Measurements were made at two isobars (10 and 40 MPa) and near the saturation curve (0.1 to 2 MPa). The range of temperature was (294 to 577) K. The total uncertainty of the thermal conductivity, pressure, temperature, and composition measurements was estimated to be less than 2%, 0.05%, 30 mK, and 0.02%, respectively. The temperature, pressure, and concentration dependence of thermal conductivity were studied. Measured values of thermal conductivity were compared with data and correlations reported in the literature. The reliability and accuracy of the experimental method were confirmed with measurements on pure water. The experimental and calculated values of thermal conductivity for pure water from the IAPWS[34] formulation show excellent agreement within their experimental uncertainties (AAD within 0.51%). The correlation equation for thermal conductivity was obtained as a function of temperature, pressure, and composition by a least-squares method from the experimental data. The AAD between measured and calculated values of thermal conductivity for solutions from this correlation equation was 1.5%. The measured thermal conductivity values of solutions were compared with the data reported in the literature by other authors. Good agreement (deviations within 0.3% to 1.0%) is found between the present measurements and the data sets reported by other authors in the literature.

Acknowledgment

I.M.A. thanks the Physical and Chemical Properties Division at the National Institute of Standards and Technology for the opportunity to work as a guest researcher at NIST during the course of this research.

Literature Cited

(1) Abdulagatov, I. M.; Magomedov, U. M. Thermal Conductivity Measurements of Aqueous $SrCl_2$ and $Sr(NO_3)_2$ Solutions in the Temperature Range Between 293 and 473 K at Pressures up to 100 MPa. *Int. J. Thermophys.* **1999**, *20*, 187−196.
(2) Abdulagatov, I. M.; Magomedov, U. B. Thermal Conductivity of Aqueous Solutions of NaCl and KCl at High Pressures. *Int. J. Thermophys.* **1994**, *15*, 401−413.
(3) Abdulagatov, I. M.; Magomedov, U. B. Thermal Conductivity of Aqueous $ZnCl_2$ Solutions at High Temperatures and High Pressures. *Ind. Eng. Chem. Res.* **1998**, *37*, 4883−4888.
(4) Abdulagatov, I. M.; Magomedov, U. B. Measurements of Thermal Conductivity of Aqueous LiCl and LiBr Solutions from 293 to 473 Pressures up to 100 MPa. *Ber. Bunsen-Ges. Phys. Chem.* **1997**, *101*, 708−711.
(5) Abdulagatov, I. M.; Magomedov, U. B. Thermal Conductivity of Aqueous $CdCl_2$ and $CdBr_2$ Solutions from 293 K to 473 K at High Pressures up to 100 MPa. *J. Chem. Eng. Data* **1997**, *42*, 1165−1169.
(6) Abdulagatov, I. M.; Magomedov, U. B. Measurements of the Thermal Conductivity of Aqueous $CoCl_2$ Solutions at Pressures up to 100 MPa by Parallel-Plate Apparatus. *J. Chem. Eng. Jpn.* **1999**, *32*, 465−471.
(7) Abdulagatov, I. M.; Magomedov, U. B. Effect of Temperature and Pressure on the Thermal Conductivity of Aqueous CaI_2 Solutions. *High Temp. − High Pressures* **2000**, *32*, 599−611.
(8) Abdulagatov, I. M.; Magomedov, U. B. Thermal Conductivity of Aqueous BaI_2 Solutions in the Temperature Range 293−473 and the Pressure Range 0.1−100 MPa. *Fluid Phase Equilib.* **2000**, *171*, 243−252.
(9) Abdulagatov, I. M.; Magomedov, U. B. Thermal Conductivity of Pure Water and Aqueous $SrBr_2$ Solutions at High Temperatures and High Pressures. *High Temp. − High Pressures* **2004**, *35/36*, 149−168.
(10) Abdulagatov, I. M.; Magomedov, U. B. Thermal Conductivity of Aqueous KI and KBr Solutions at High Temperatures and High Pressures. *J. Solution Chem.* **2001**, *30*, 223−235.
(11) Abdulagatov, I. M.; Akhmedova-Azizova, L. A.; Azizov, N. D. Thermal Conductivity of Aqueous $Sr(NO_3)_2$ and $LiNO_3$ Solutions at High Temperatures and High Pressures. *J. Chem. Eng. Data* **2004**, *49*, 688−704.
(12) Azizov, N. D. Thermal Conductivity of Aqueous Solutions of Li_2SO_4 and $Zn(NO_3)_2$. *Russ. High Temp.* **1999**, *37*, 649−651.
(13) Akhundov, T. C.; Iskenderov, A. I.; Akhmedova, L. A. Thermal Conductivity of Aqueous Solutions of $Ca(NO_3)_2$. *Izv. Vuzov, ser. Neft i Gas* **1994**, *3*, 49−52.
(14) Akhundov, T. C.; Iskenderov, A. I.; Akhmedova, L. A. Thermal Conductivity of Aqueous Solutions of $Mg(NO_3)_2$. *Izv. Vuzov, ser. Neft i Gas* **1995**, *1*, 56−58.
(15) Abdulagatov I. M., Magomedov U. B. *Thermal Conductivity of Aqueous Solutions of $CaCl_2$ and $MgCl_2$ at High Pressures*. In Proceedings of the 12th International Conference on the Properties of Water and Steam; White, H. J., Sengers, J. V., Neumann, D. B., Bellows, J. C., Eds.; Begell House: New York. 1995; pp 549−557.
(16) Rastorguyev, Y. L.; Grigoryev, B. A.; Safronov, G. A.; Ganiev, Y. A. *Thermal Conductivity of Aqueous Solutions of Alkali Metals Halides*. In Proceedings of the 10th International Conference on the Properties of Steam; Sychev, V. V., Aleksandrov, A. A., Eds.; Mir: Moscow, 1984; Vol. 2, pp 210−218.
(17) El'darov, V. S. Thermal Conductivity of Aqueous Solutions of Nitrate Salts. *Russ. J. Phys. Chem.* **1986**, *60*, 603−605.
(18) Abdullaev, K. M.; El'darov, V. S.; Manafov, S. M. Effect of Pressure on the Thermal Conductivity of Aqueous Electrolyte Solutions. *Izv. Vyssh. Ucheb. Zaved., ser. Energetika* **1981**, *5*, 67−71.
(19) Magomedov, U. B. Thermal Conductivity of Aqueous Salt Solutions at High Temperatures and High Pressures. In *Geothermic, Geology, and Thermophysics*. DSC, IPG: Makhachkala, 1992; pp 168−187.
(20) Safronov, G. A.; Kosolap, Y. G.; Rastorguev, Y. L. *Experimental Studies of the Thermal Conductivity of Binary Aqueous Solutions of Electrolytes*; Deposit. VINITI SSSR, Dep. no. 4262-B90, 1990; pp 1−29.
(21) Safronov, G. A.; Kosolap, Y. G.; Rastorguev, Y. L. *Experimental Study of the Thermal Conductivity of Electrolytes*; Groznyi Oil Institute: Groznyi, 1990; pp 1−28.
(22) Aseyev, G. G. *Electrolytes: Properties of Solutions. Methods for Calculation of Multicomponent Systems and Experimental Data on Thermal Conductivity and Surface Tension.* Begell-House Inc.: New York, 1998.
(23) Zaitsev, I. D.; Aseyev, G. G. *Physical and Chemical Properties of Binary and Multicomponent Nonorganic Solutions*;, Khimiya: Moscow, 1988.
(24) Zaitsev, I. D.; Aseyev, G. G. *Properties of Aqueous Solutions of Electrolytes*; CRC Press: Boca Raton, FL, 1992.
(25) Riedel, L. The Heat Conductivity of Aqueous Solutions of Strong Electrolytes. *Chem. -Ing. -Tech.* **1951**, *23*, 59−64.

(26) Kapustinskii, A. F.; Ruzavin, I. I. Thermal Conductivity of Aqueous Electrolyte Solutions. Experimental Study of the Aqueous Solutions of KF, LiCl, NaCl, KCl, RbCl, CsCl, NaBr, KBr, NaJ, KJ, Na_2SO_4, $BeSO_4$, $MgCl_2$, $CaCl_2$, and $AlCl_3$. *Russ. J. Phys. Chem.* **1955**, *29*, 2222−2226.
(27) Vargaftik, N. B.; Os'minin, Yu. P. Thermal Conductivity of Aqueous Salt, Acid, and Alkali Solutions. *Teploenergetika* **1956**, *7*, 15−16.
(28) Barratt, T.; Nettlrton, H. R. In *International Critical Tables*; McGraw-Hill: New York, 1929; Vol. 5.
(29) DiGuilio, R. M.; Lee, R. J.; Jeter, S. M.; Teja, A. S. Properties of Lithium Bromide − Water Solutions at High Temperatures and Concentrations I: Thermal Conductivity. *ASHRAE Trans.* **1990**, *96*, 702−708.
(30) DiGuilio, R. M.; Teja, A. S. Thermal Conductivity of Aqueous Salt Solutions at High Temperatures and High Concentrations. *Ind. Eng. Chem. Res.* **1992**, *31*, 1081−1085.
(31) Bleazard, J. G.; DiGuilio, R. M.; Teja A. S. Thermal Conductivity of Lithium Bromide-Water Solutions. *AIChE Symp. Ser.* **1994**, *298*, 23−28.
(32) Bleazard, J. G.; Teja, A. S. Thermal Conductivity of Electrically Conducting Liquids by the Transient Hot-Wire Method. *J. Chem. Eng. Data* **1995**, *40*, 732−737.
(33) Chiquillo, A. *Measurements of the Relative Thermal Conductivity of Aqueous Salt Solutions with a Transient Hot-Wire Method*. Juris Druck+Verlag: Zurich, 1967.
(34) Kestin, J.; Sengers, J. V.; Kamgar-Parsi, B.; Levelt Sengers, J. M. H. Thermophysical Properties of Fluid H_2O. *J. Phys. Chem. Ref. Data* **1984**, *13*, 175−189.
(35) Gershuni, G. Z. Thermal Convection in the Space Between Vertical Coaxial Cylinders. *Dokl. Akad. Nauk USSR* **1952**, *86*, 697−698.
(36) Healy, J.; de Groot, J. J.; Kestin, J. The Theory of the Transient Hot-Wire Method for Measuring Thermal Conductivity. *Physica C* **1976**, *82*, 392−408.
(37) Ramires, M. L. V.; Nieto de Castro, C. A.; Nagasaka, Y.; Nagashima, A.; Assael, M. J.; Wakeham, W. A. Standard Reference Data for the Thermal Conductivity of Water. *J. Phys. Chem. Ref. Data* **1995**, *24*, 1377−1381.

Received for review May 19, 2004. Accepted July 26, 2004.

JE049814B